Observation of excited state absorption in the V-Cr Prussian blue analogue

Observation of excited state absorption in the V-Cr Prussian blue analogue

Luke Hedley,[1] Michael D. Horbury,[2] Florian Liedy,[1] J. Olof Johansson*,[1]
[1] *EaStCHEM, School of Chemistry, University of Edinburgh, David Brewster Road, EH9 3FJ, UK*
[2]Department of Chemistry, University of Warwick, Gibbet Hill, CV4 7AL, Coventry, UK
*Corresponding author. Email address: olof.johansson@ed.ac.uk

Abstract

We present femtosecond transient transmission measurements of thin films of the $V^{II/III}$-Cr^{III} Prussian blue analogue (V-Cr PBA) in the spectral range 330−675nm after exciting the ligand-to-metal charge-transfer transition (LMCT) at 400nm. A global analysis including three decay-times of τ_1=230fs, τ_2=1.38ps and τ_3>>2ns could satisfactory describe the data. We observed an excited state absorption (ESA) at 345nm, which was attributed to a charge-transfer transition from the ^{2}E state on the Cr ions after fast intersystem crossing from the quartet manifold. An additional weak and short-lived ESA at 455nm was also observed and was tentatively attributed to the initially populated ^{4}LMCT state.

Keywords: ultrafast spectroscopy; Prussian blue analogues; charge-transfer transitions; functional materials; thin films; spectroelectrochemistry

1. Introduction

Smart materials can be controlled using external perturbations to switch their electrical, optical and magnetic properties. Understanding the photophysics of charge-transfer (CT) transitions in these materials provides an interesting problem connecting light, charge and spin dynamics. For example, spin crossover (SCO) systems, which can be optically switched from low-spin to high-spin states, have been extensively studied for a number of years [1–4]. In Fe(II) complexes, where the SCO process is from the singlet ground state (S = 0) to a quintet meta-stable state (S = 2), it has been found that spin switching can occur in less than 100 fs [2,5,6].

Progress in this area can be important for future photonic devices combining optical control of electrical and magnetic properties. For achieving optical control of magnetically ordered materials, Prussian blue analogues (PBAs) have been extensively studied during the last twenty years [7,8]. These materials have a rock-salt structure with transition metal ions linked by cyanide bridging ligands (Fig. 1, inset). In particular, the V-Cr PBA is an interesting model system because of its high magnetic ordering temperature above room temperature [9–12]. The V-Cr PBA also displays interesting proton conductive [13], photomagnetic [14] and electrochromic [15,16] properties. There have been few ultrafast studies to date on PBAs in general [17–22] to probe the initial fs−ps dynamics after photoexcitation. The relatively large number of studies on the V-Cr PBA's static optical and magnetic properties means that it provides an interesting system for understanding both charge and spin dynamics after fs laser excitation in these systems. Here, we have explored transient transmission spectroscopy with the aim to study intermediate states important for the fast intersystem crossing (ISC) previously reported for various Cr-containing complexes and materials [21,23–28].

The optical spectrum of the V-Cr PBA (Fig. 1) is dominated by metal-to-metal charge-transfer (MMCT) transitions in the visible and ligand-to-metal (LMCT) and metal-to-ligand (MLCT) CT transitions in the UV. The MMCT transition takes place between localised electrons in t_{2g} orbitals on the Cr and V ions (Fig. 2). A recent study employed ultrafast magneto-optical (MO) methods to directly study photo-induced spin dynamics in the V-Cr PBA after exciting at the LMCT transition [21]. The excitation in films of the V-Cr PBA appears to take place on localised sites in the lattice during the first few hundred fs [21], similarly to what is also observed in SCO crystals of Fe(II) complexes [29,30]. The ultrafast dynamics of $Cr(acac)_3$ in liquids, which has been extensively studied by Juban and McCusker [23], is therefore relevant for understanding the dynamics in thin films of the V-Cr PBA. The LMCT pump transition corresponds to transferring an electron from a CN^- ligand to a Cr(III) site, thereby photo-reducing the ion transiently to a Cr(II) oxidation state (Fig. 2 (b)). Back-electron transfer subsequently occurs very quickly and the Cr(III) oxidation state is formed again on a sub-100 fs timescale, similarly

to the decay of the MLCT state in Fe(II) SCO complexes in solution or crystals. However, a fraction of the Cr(III) sites are now formed in the ^{2}E doublet state via fast ISC from the quartet manifold (Fig. 2 (c)). The MO measurements could detect the formation of this doublet state on the Cr ion due to the change in the super-exchange interaction of this magnetically ordered material taking place as a result of the corresponding spin flip associated with the ISC [21]. The model describing this dynamics was inferred from the model developed by Juban and McCusker, who studied isolated $Cr(acac)_3$ ions in solution where a spectral broadening and red-shift of the excited-state absorption from the ^{2}E state could be followed and compared to ns results [23,25]. More recent studies using time-resolved IR techniques have shown that a relatively large fraction of the ^{2}E state population decays back to the quartet manifold via back-ISC [24,27].

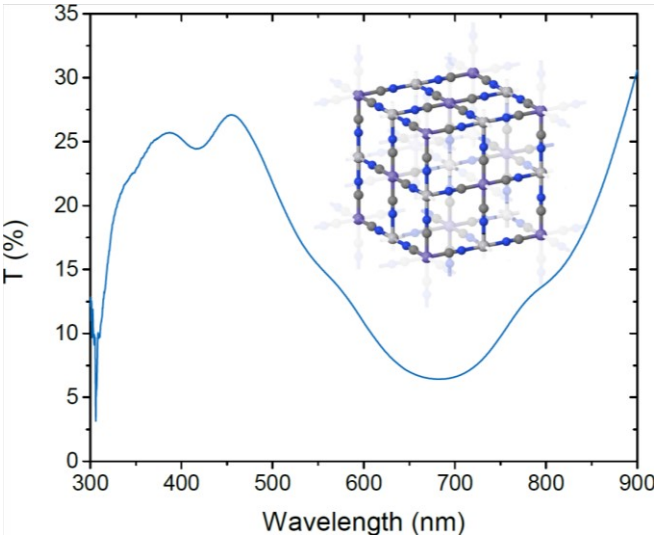

Fig. 1: Static transmission spectrum of the V-Cr PBA. The loss of transmission in the visible region is due to MMCT transitions between Cr(III)-V(II) at 540 nm (seen as a shoulder) and Cr(III)-V(III), which occurs closer to 670 – 690 nm for this particular film. LMCT/MLCT transitions occur ≤ 400 nm. Inset shows idealised crystal structure of the V-Cr PBA lattice.

To understand the pathways involved in the fast ISC process, it is important to study the initially populated CT state, corresponding to the reduced Cr ion (Fig. 2 (b)). We label this state ^{4}LMCT, where the spin multiplicity corresponds to the total spin of the Cr ion and ligand to

highlight that the total spin is conserved after absorbing a pump photon. In the previous ultrafast magneto-optical study, an increase in absorption at 480 nm could just be discerned at early delay times and was tentatively assigned to an ESA from the initially excited CT state [21]. It should be noted that the LMCT state in $Cr(acac)_3$ in solution has previously been shown to decay in less than 50 fs [23], making this state difficult to detect with the ca. 250 fs cross-correlation used in the magneto-optical study. Furthermore, the increase in absorption took place just at the blue edge of the white-light supercontinuum. In addition to the problem with the short-lived nature of the ^{4}LMCT state, one still must find a clear optical signature of this state, which is not always trivial. In order to approach this more general problem, spectroelectrochemistry and transient absorption have previously been used to identify and study the dynamics of charge-transfer excited states in several systems (e.g. [31] and references therein). Inspired by our recent spectroelectrochemical study on thin films of the V-Cr PBA [16], we have in this letter investigated if a similar approach would be feasible. In the spectroelectrochemical study, we found that a new optical absorption peak arises at *ca*. 465 nm when the films were electrochemically reduced. This process corresponds to the reduction of $[Cr^{III}(CN)_6]^{3-}$ sites to $[Cr^{II}(CN)_6]^{4-}$ in the PBA lattice, which in principle is similar to the LMCT photoexcitation process when the Cr sites are reduced by the transfer of an electron from the ligands. The absorption from the reduced Cr sites was attributed to a red-shift of a MLCT transition from Cr(II) to empty π* ligand orbitals, due to the increased energy of Cr(II) compared to Cr(III), pushing it closer in energy to the empty ligand orbitals. However, an ESA signal from the ^{2}E or ^{4}LMCT states has to date not been clearly observed in films of the V-Cr PBA. In this letter, we present a transient transmission study of the V-Cr PBA with the aim to observe ESA from the ^{2}E state and to capture the short-lived ^{4}LMCT state on the photo-reduced Cr ions in the PBA lattice by probing with a wider spectral range, spanning 330 − 675 nm. We were able to observe a transient absorption centred at 345 nm, which we attribute to the ^{2}E state. In addition, we also observed a weak and short-lived ESA at 455 nm, which is consistent with the spectroelectrochemical measurements of reduced Cr ions. The measured lifetime was less than 50 fs, in agreement with the short lifetime previously assigned to the

LMCT state. Our findings are consistent with the model of fast ISC to the ^{2}E state after pumping the ^{4}LMCT state.

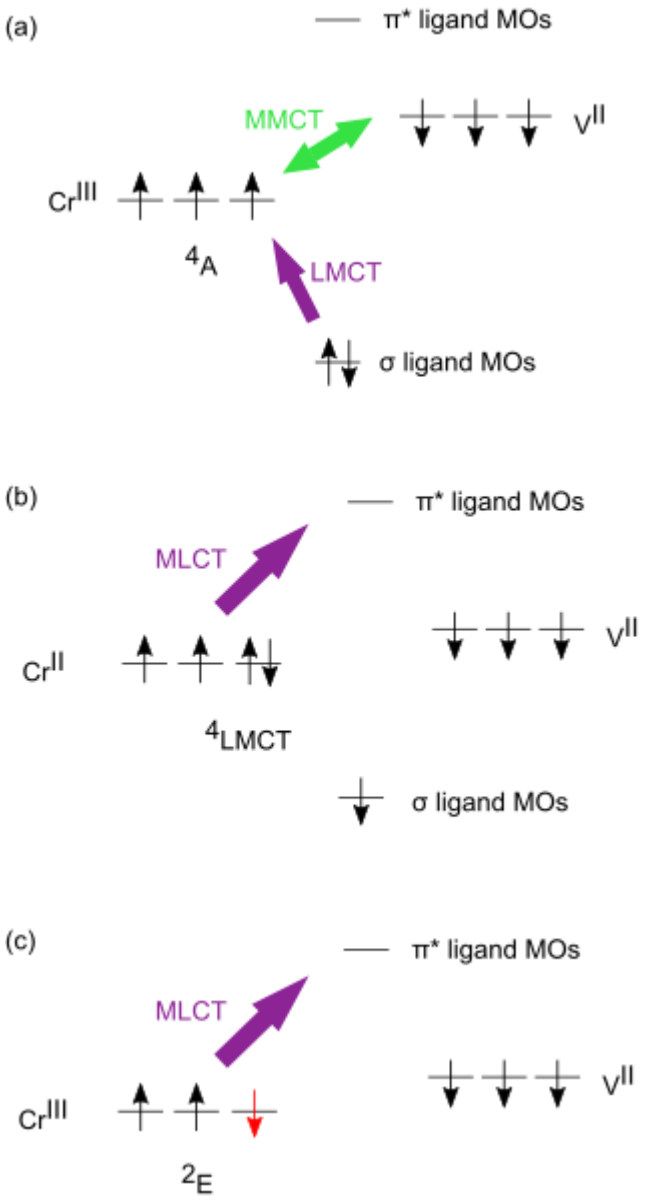

Fig. 2: Schematic diagram of orbital energy levels and optical transitions in the V-Cr PBA. (a) Ground-state electronic configuration, where only the t_{2g} orbitals on the metal ions are shown (e_g orbitals are not populated). Filled and empty CN^- ligand orbitals are also shown. (b) After pumping at the LMCT, the Cr ion is reduced to Cr(II). The energy of the electrons localised on the ion is therefore increased closer to the empty π ligand orbitals. This causes a red-shift of the MLCT transition. Spin multiplicity of ^{4}LMCT refers to the total spin of the system in this case and implies spin is conserved after the LMCT excitation. (c) After the decay of the ^{4}LMCT*

state and back-electron transfer, the Cr is formed as Cr(III) again. After ISC to the ^{2}E state, one of the electrons on the Cr ion has changed its spin projection. Note that the transition energy of the MLCT is larger in (c) than (b) because the ^{2}E state on Cr(III) is lower in energy than the ^{4}LMCT state on Cr(II).

2. Methods

The synthesis of the films followed the procedure by Ohkoshi et al. [32] and has been described in more details in ref. [16]. In short, cleaned glass substrates coated with fluorine-doped tin-oxide (FTO) were held under a constant potential of −1.2 V for 300 s in a solution of $K_3[Cr^{III}(CN)_6]$ and VCl_3 at 25 mM concentrations in an electrolytic solution of KCl (1.0 M) in water. The films are air sensitive so all the synthesis was carried out in a nitrogen environment. The films were dried in nitrogen flow and subsequently sealed with a cover glass slip and cyanoacrylate glue. In order to estimate the film thickness, we compared the transmittance with our previous study and could estimate the film thickness to be 600 ± 50 nm [16].

The transient absorption setup based at Warwick University has been described previously [33,34]. Briefly, the white-light continuum is generated in a CaF_2 plate and the probe spectrum is detected using an Avantes fibre-coupled spectrometer (AvaSpec-ULS1650F). The pump beam was relatively defocussed with a beam waist of 1.5 mm. The pump pulse energy was 400 nJ, which therefore corresponds to a fluence in the focal region of 22 μJ/cm^2. We monitored the pump-probe signal at 0 and 1000 fs delays between each scan to check for any film degradation. However, with the lower pump energy used, we could not observe any long-term changes to the signal. The pump pulse duration was 80 fs and the pump-probe beam angle was less than four degrees. The obtained transient transmittance was analysed in a sequential global-fit procedure using the Glotaran software [35].

3. Results and discussion

3.1. Overview of broadband transient transmission results

The transient transmission spectra obtained after pumping at 400 nm are presented in Fig.3 (a) as a function of pump-probe delay up to 5 ps. The time-delays were scanned up to 1.8 ns but we found that most of the dynamics had reached a plateau after ca. 5 ps, in agreement with previous work [21]. We therefore only show time-delays up to 5 ps in the 2D data. Kinetic traces for selected wavelengths for full delay times are presented in the Fig. 2 (c). The signal around 400 nm observed in Fig.2 (a) is due to scattered pump light reaching the detector. In this time window this data is characterised by two specific features, namely a bleach, or increase of transmittance, for wavelengths above ca. 475 nm and a decrease in transmittance below this wavelength. The results in the visible region (500 – 700 nm) are similar to what was previously observed, i.e. bleach of the MMCT after pumping at the LMCT [21]. It should be noted that the position of the ground-state bleach (GSB) is red-shifted compared to our previous study (ca. 660 nm). However, we believe this is due to variability of the films used since the position of the MMCT can depend on the specific stoichiometry and morphology of the films, which can be different as a result of slightly different electrochemical deposition conditions [12]. The peak of the MMCT for the film in this study do indeed occur at 680 nm, as seen in Fig. 1. The UV part of the spectrum was previously unexplored and so the finding of a decrease in transmittance in this spectral range is new. Although we have not measured the change in reflectance, we attribute the reduced transmittance to an ESA, which provides an interesting avenue to directly explore the nature of the excited state instead of solely relying on the GSB. This feature is discussed further in Section 3.2. The data was analysed using a sequential global fit procedure and three time-constants were found to describe the results adequately. We found two timescales of τ_1 = 230 ± 40 fs and τ_2 = 1.38 ± 0.04 ps. The third time-constant was larger than 2 ns and was thus equivalent to a constant offset.

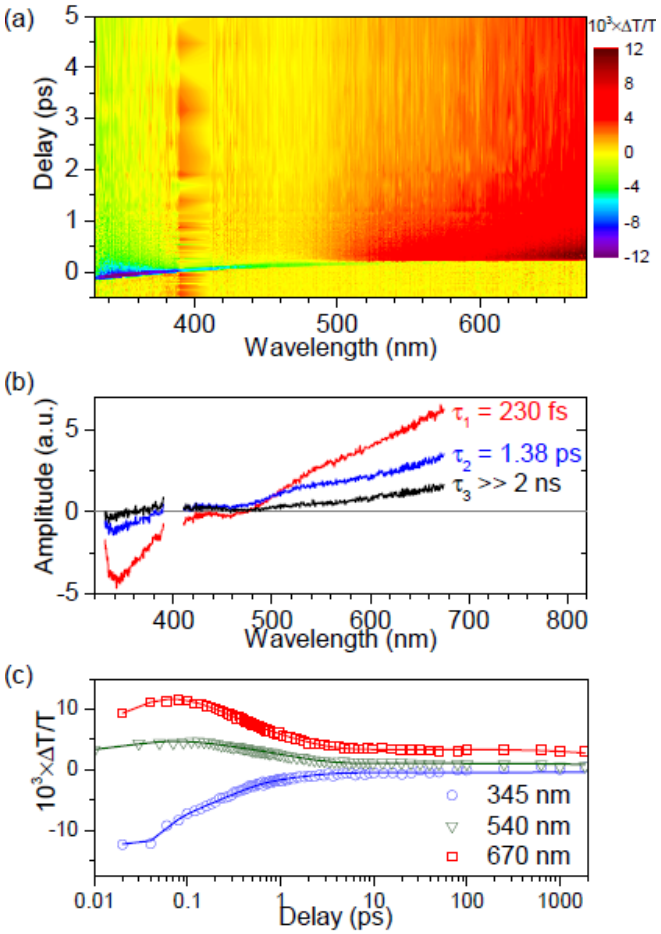

Fig. 3: Ultrafast dynamics of the V-Cr PBA after pumping at the LMCT transition. (a) Transient transmission results as a function of pump-probe delay time and wavelength. The signal at 400 nm is due to scattered pump light. The data has not been corrected for the white-light chirp (this has been done in all subsequent analysis). Fitted evolution associated difference spectra (EADS) from the global analysis are presented in (b). The pump signal at 400 nm has been removed for clarity. (c) Kinetic traces at selected wavelengths are shown on a semi logarithmic scale. Points are experimental data whereas solid lines are the results from the global analysis. The kinetic traces were averaged over a 10 nm bandwidth.

3.2 Excited state absorption in the UV

The ESA in the UV can be seen in both the 2D transient transmittance data and the evolution associated difference spectra (EADS) resulting from the global fit in Fig. 3 (a) and (b), respectively. Due to the larger spectral range, available with the CaF_2 supercontinuum

generation, we were able to observe an ESA in the wavelength region around 330 – 350 nm. This ESA has previously not been observed for the V-Cr PBA. We have also carried out a measurement on the glass-substrate alone (including FTO, superglue, and coverslip) but did not observe any ESA in this wavelength range (besides from the coherent signal at time-zero). The ESA was also present in the global analysis, but was more dominated by the fast decay component (τ_1 = 230 fs). The larger relative amplitude component of the fast channel compared to the MMCT bleach is clearly visible during the first 500 fs, which is demonstrated in Fig. 4. We have also shown the dynamics at 540 nm, corresponding to the MMCT of V^{II}-Cr^{III}, for comparison in Fig. 4. There is a constant plateau in the ESA decay similarly to the MMCT bleach, although it is just above the noise-level, as modelled by the non-zero τ_3 component of the global analysis.

To attempt to identify the state giving rise to the UV-ESA, one must consider the model discussed in the introduction (Fig. 2). The spectral shapes of the bleach region and the ESA are rather similar for the three different time-constants obtained in the global analysis. This implies that there is not a large change in the electronic character of the excited state after the initial dynamics occurring during the rise time of the pump pulse. This argument was used by Juban and McCusker to conclude that the ^{2}E state was formed on a very fast timescale (less than 100 fs) because the few-fs transient absorption spectrum matched that of the ns spectrum. Based on the physical model, whereby the intermediate ^{4}LMCT state decays with a 20 – 50 fs time-constant to the ^{2}E state, we attribute the ESA to the ^{2}E state. Due to the short lifetime of the ^{4}LMCT state, we do not see any delayed onset of the UV-ESA and we conclude that the ^{2}E state is populated during the rise-time of the laser pulses. The transient transmission signal appears to be rather strong and comparable to the MMCT bleach. This could potentially suggest that it is a CT transition that is giving rise to the ESA in the V-Cr PBA instead of a metal-centred transition (d-d transition). The ESA could therefore originate from a red-shifted MLCT transition, in analogy to the assignment of the additional absorption of the reduced Cr sites observed in our recent spectroelectrochemistry study as discussed in the

Introduction [16]. The red-shifted MLCT state in Cr(II) in the spectroelectrochemical study was observed at 465 nm while the ESA in the ^{2}E state in this study was observed at ca. 345 nm. The MLCT transition energy difference is reasonable because it is expected that the ^{2}E state is lower in energy than the reduced Cr(II).

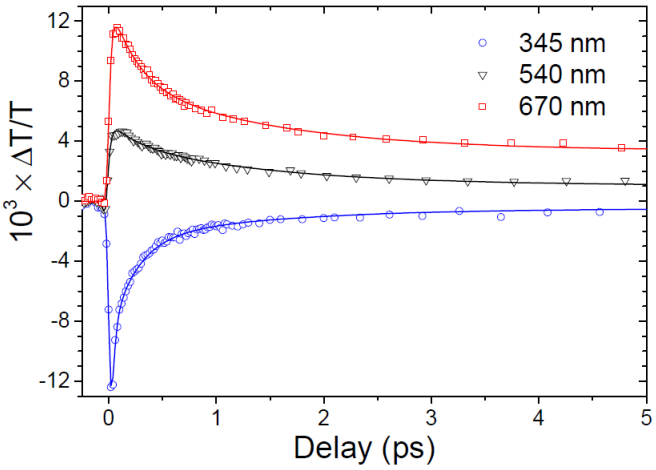

Fig. 4: Kinetic traces for selected wavelengths up to 5 ps (full time-delays are shown in Fig. 3 (c)). Points are experimental data whereas solid lines are the results from the global analysis. The kinetic traces were averaged over a 10 nm bandwidth.

A fraction of the ^{2}E state population will decay back to the quartet manifold via back-ISC on a sub-100 fs timescale [24,25,27]. The EADS from the global analysis below 350 nm show a non-zero component of the τ_3>>ns component. This plateau corresponds to the fraction of the population trapped in the ^{2}E state. However, this fraction is smaller than that expected from the plateau of the MMCT bleach and the signal above ca. 100 ps is in the noise level. It is therefore difficult to extract information about the plateau observed so clearly for the MMCT bleach. The τ_1 to τ_2 ratio is large in this wavelength range, which indicates that the majority of the ^{2}E state population decays back to the quartet manifold on a 230 fs timescale. The 1.38 ps timescale then corresponds to vibrational cooling of the trapped ^{2}E states. These new measurements therefore indicate that the ^{2}E population after a few ps is lower than that estimated from the GSB.

3.3. Observation of short-lived ^{4}LMCT state

In order to test the hypothesis that the ^{4}LMCT state could be observed during early time delays in the blue region of the spectrum, the transient spectra at early time-delays were more closely inspected in the narrow spectral range 420 – 480 nm. The corresponding result of the global analysis in this spectral region for the two short time-constants are shown in Fig. 5 (a). The main difficulty with observing any signal at 455 nm is that this wavelength region falls between the rather intense ESA at shorter wavelength and the GSB at longer wavelengths. Nevertheless, there is an additional absorption feature that does not appear to be connected to the ESA in the UV or the GSB in the visible. The slight decrease in transmission, corresponding to increase in absorption, can be seen at 455 nm in Fig. 5 (a). The spectral position of this peak is indeed close to 465 nm, which is measured in the spectroelectrochemical measurements [16]. The decay of this additional absorption feature is short-lived and so it becomes difficult to extract the time dynamics from the coherent artefact from the glass substrate and the chirp of the white-light continuum (Fig. S1). A shorter time-constant than 230 fs should in principle be included in the global analysis, but based on the aforementioned arguments, it becomes difficult to reliably extract relevant data from the global analysis for these conditions. We have therefore plotted the experimental data, averaged over a 10 nm wavelength range at 434, 455 and 465 nm in Fig. 5 (b). For these three wavelengths, the coherent signal peak from the glass substrate can be seen as a decrease in transmittance around time-zero with a FWHM corresponding to the instrumental response function ($\Delta t_{FWHM} = 50\ fs$). However, for the transient at 455 nm there is clearly a signal persisting for about 20 – 50 fs longer than the glass-substrate signal. Because the transient at 455 nm stands out from the adjacent wavelengths and is observed in the global analysis in Fig. 5 (a), we exclude the possibility that this signal is simply an ultrafast artefact. However, further measurements using even shorter laser pulses are needed to study the ESA signal in more detail.

We tentatively assign the short-lived ESA at 455 nm to the ^{4}LMCT state. Taking into account that the spectral position is in close agreement with spectroelectrochemical measurements, the appearance of the ESA at 345 nm from the ^{2}E state at early time delays (and that this state is populated from the ^{4}LMCT state) and the expected short lifetime, we believe that a tentative assignment of the ^{4}LMCT state is reasonable. Based on the assignment in the spectroelectrochemical study mentioned in the introduction, we attribute the ESA to a MLCT transition, which is red-shifted with respect to the ground state absorption due to the higher energy of the photo-reduced Cr(II) compared to Cr(III). Of course, the spectral position in the transient transmission data does not necessarily have to be the same as in the spectroelectrochemical data because in that case the Cr ions are reduced by electrons from the electrode and subsequently K^+ counter ions (supplied from the electrolyte) are inserted into the films to maintain the charge-balance. In contrast, the transient transmission measurements are not carried out in an electrolyte and the source of electrons is not from an electrode, but rather from the cyanide ligand. We use this reason to justify the short lifetime of the photoexcited ^{4}LMCT state compared to the stabilised lifetime of the electrochemically reduced Cr ions. The short lifetime of the intermediate ^{4}LMCT is in agreement with that measured in $Cr(acac)_3$ by Juban and McCusker, who observed a time-constant of 50 ± 20 fs [23].

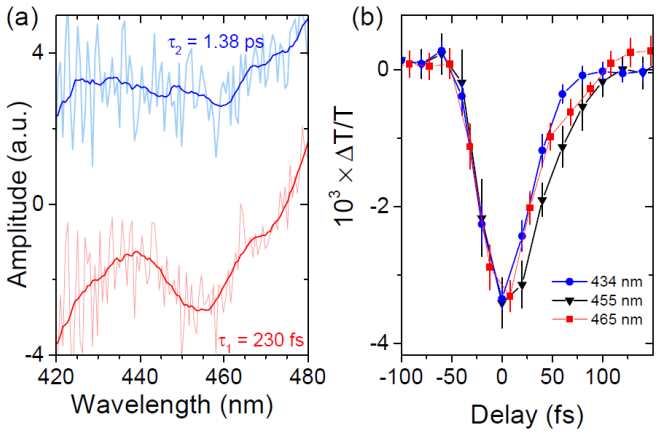

Fig. 5: Identification of intermediate charge-transfer state on photo-reduced Cr(II) sites. (a) The EADS from Fig. 3 (a) for τ_1 = 230 fs and τ_2 = 1.38 ps in a narrower spectral range. Due to

the weak signal in this range, the EADS were smoothed to identify any additional absorption (corresponding to reduced transmittance). The ^{4}LMCT ESA was attributed to the drop in the transmission coefficient in the EADS *at 455 nm for the faster τ_1 = 230 fs component. (b) The kinetic traces close to time-zero for three wavelength regions averaged over a 10 nm bandwidth. The error bars are from the standard deviation of the averaged 10 nm wavelength region. The decrease in transmission is due to the coherent signal of the glass substrate. The lingering signal at 455 nm is attributed to the short-lived ^{4}LMCT state.*

4. Conclusion

We conclude that the experimental results presented here are consistent with the formation of a short-lived ^{4}LMCT state upon exciting at the LMCT transition, which subsequently decays to the ^{2}E state on a sub-100 fs timescale. This state is characterised by a MMCT bleach in the visible and an ESA in the UV at 345 nm. The decay of the observed ESA signal for the ^{2}E state at 345 nm, indicates that most of the ^{2}E state population undergoes back-ISC on a 230 fs timescale but some part of the population is trapped in the ^{2}E state. We could also observe a weak signal that was tentatively assigned to the short-lived ^{4}LMCT state on the Cr ions, which is populated by the pump pulse. An ESA associated with this state was observed at 455 nm and could be due to a red-shifted MLCT transition, which is in good agreement with spectroelectrochemistry of reduced Cr sites in the V-Cr PBA lattice. The ^{4}LMCT state subsequently decays to the ^{2}E state. The fast decay implies that the ISC happens on the same fast timescale limited by the instrument-response function of ca. 50 fs. The ESA signals observed for both states should provide a more direct approach to further study the dynamics in this important molecular magnet without relying on the ground-state bleach. The results show that using spectroelectrochemistry to study femtosecond charge-transfer dynamics in PBAs is a powerful method and should be applicable to other inorganic coordination polymers cast in thin films.

Acknowledgements

This work was supported by funding from the Royal Society of Edinburgh and EPSRC (studentship to LH). M. D. H. thanks the Leverhulme Trust for postdoctoral funding. The authors thank V. Stavros for use of the laser lab and N. Robertson for the use of the potentiostat for making films. J. O. J. is a Royal Society of Edinburgh/BP Trust research fellow.

References

[1] S. Decurtins, P. Gütlich, C.P. Köhler, H. Spiering, A. Hauser, Light-induced excited spin state trapping in a transition-metal complex: The hexa-1-propyltetrazole-iron (II) tetrafluoroborate spin-crossover system, Chem. Phys. Lett. 105 (1984) 1–4. doi:10.1016/0009-2614(84)80403-0.

[2] J.E. Monat, J.K. McCusker, Femtosecond excited-state dynamics of an iron(II) polypyridyl solar cell sensitizer model, J. Am. Chem. Soc. 122 (2000) 4092–4097. doi:10.1021/ja992436o.

[3] A. Cannizzo, C.J. Milne, C. Consani, W. Gawelda, C. Bressler, F. van Mourik, M. Chergui, Light-induced spin crossover in Fe(II)-based complexes: The full photocycle unraveled by ultrafast optical and X-ray spectroscopies, Coord. Chem. Rev. 254 (2010) 2677–2686. doi:10.1016/j.ccr.2009.12.007.

[4] M. Halcrow, Spin-Crossover Materials: Properties and Applications, Wiley VCH, 2013.

[5] G. Auböck, M. Chergui, Sub-50-fs photoinduced spin crossover in [Fe(bpy)3]2+, Nat. Chem. 7 (2015) 629–633. doi:10.1038/nchem.2305.

[6] H.T. Lemke, K.S. Kjær, R. Hartsock, T.B. van Driel, M. Chollet, J.M. Glownia, S. Song, D. Zhu, E. Pace, S.F. Matar, M.M. Nielsen, M. Benfatto, K.J. Gaffney, E. Collet, M. Cammarata, Coherent structural trapping through wave packet dispersion during photoinduced spin state switching, Nat. Commun. 8 (2017) 15342. doi:10.1038/ncomms15342.

[7] M. Verdaguer, G.S. Girolami, Magnetic Prussian Blue Analogs, in: J.S. Miller, M. Drillon (Eds.), Magn. Mol. to Mater., Wiley-VCH Verlag GmbH & Co. KGaA, Weinheim, Germany, 2005: pp. 283–346. doi:10.1002/9783527620548.ch9d.

[8] S. Ohkoshi, H. Tokoro, Photomagnetism in Cyano-Bridged Bimetal Assemblies, Acc. Chem. Res. 45 (2012) 1749–1758. doi:10.1021/ar300068k.

[9] S. Ferlay, T. Mallah, R. Ouahès, P. Veillet, M. Verdaguer, A room-temperature organometallic magnet based on Prussian blue, Nature. 378 (1995) 701–703. doi:10.1038/378701a0.

[10] Ø. Hatlevik, W.E. Buschmann, J. Zhang, J.L. Manson, J.S. Miller, Enhancement of the Magnetic Ordering Temperature and Air Stability of a Mixed Valent Vanadium Hexacyanochromate(III) Magnet to 99 °C (372 K), Adv. Mater. 11 (1999) 914–918. doi:10.1002/(SICI)1521-4095(199908)11:11<914::AID-ADMA914>3.0.CO;2-T.

[11] S.M. Holmes, G.S. Girolami, Sol−Gel Synthesis of KV II [Cr III (CN) 6]·2H 2 O: A Crystalline Molecule-Based Magnet with a Magnetic Ordering Temperature above 100 °C, J. Am. Chem. Soc. 121 (1999) 5593–5594. doi:10.1021/ja990946c.

[12] R. Garde, F. Villain, M. Verdaguer, Molecule-Based Room-Temperature Magnets: Catalytic Role of V(III) in the Synthesis of Vanadium−Chromium Prussian Blue Analogues, J. Am. Chem. Soc. 124 (2002) 10531–10538. doi:10.1021/ja020528z.

[13] S.-I. Ohkoshi, K. Nakagawa, K. Tomono, K. Imoto, Y. Tsunobuchi, H. Tokoro, High Proton Conductivity in Prussian Blue Analogues and the Interference Effect by Magnetic Ordering, J. Am. Chem. Soc. 132 (2010) 6620–6621. doi:10.1021/ja100385f.

[14] K.D. Bozdag, J.-W. Yoo, N.P. Raju, A.C. McConnell, J.S. Miller, A.J. Epstein, Optical control of magnetization in a room-temperature magnet: V-Cr Prussian blue analog, Phys. Rev. B. 82 (2010) 94449. doi:10.1103/PhysRevB.82.094449.

[15] M. Verdaguer, M. Glavez, R. Garde, C. Desplanches, Electrons at Work in Prussian

Blue Analogues, Electrochem. Soc. Interface. 11 (2002) 28.

[16] L. Hedley, N. Robertson, J.O. Johansson, Electrochromic Thin Films of the V-Cr Prussian Blue Analogue Molecular Magnet, Electrochim. Acta. 236 (2017) 97–103. doi:10.1016/j.electacta.2017.03.166.

[17] D.C. Arnett, P. Voehringer, N.F. Scherer, Excitation Dephasing, Product Formation, and Vibrational Coherence in an Intervalence Charge-Transfer Reaction, J. Am. Chem. Soc. 117 (1995) 12262–12272. doi:10.1021/ja00154a028.

[18] H. Kamioka, Y. Moritomo, W. Kosaka, S. Ohkoshi, Dynamics of charge-transfer pairs in the cyano-bridged Co2+-Fe3+ transition-metal compound, Phys. Rev. B. 77 (2008) 180301. doi:10.1103/PhysRevB.77.180301.

[19] D. Weidinger, D.J. Brown, J.C. Owrutsky, Transient absorption studies of vibrational relaxation and photophysics of Prussian blue and ruthenium purple nanoparticles., J. Chem. Phys. 134 (2011) 124510. doi:10.1063/1.3564918.

[20] A. Asahara, M. Nakajima, R. Fukaya, H. Tokoro, S. Ohkoshi, T. Suemoto, Ultrafast dynamics of reversible photoinduced phase transitions in rubidium manganese hexacyanoferrate investigated by midinfrared CN vibration spectroscopy, Phys. Rev. B. 86 (2012) 195138. doi:10.1103/PhysRevB.86.195138.

[21] J.O. Johansson, J.-W. Kim, E. Allwright, D.M. Rogers, N. Robertson, J.-Y. Bigot, Directly probing spin dynamics in a molecular magnet with femtosecond time-resolution, Chem. Sci. 7 (2016) 7061–7067. doi:10.1039/C6SC01105E.

[22] S. Zerdane, M. Cammarata, L. Balducci, R. Bertoni, L. Catala, S. Mazerat, T. Mallah, M.N. Pedersen, M. Wulff, K. Nakagawa, H. Tokoro, S. Ohkoshi, E. Collet, Probing transient photoinduced charge-transfer in Prussian Blue Analogues with time-resolved XANES and optical spectroscopy, Eur. J. Inorg. Chem. (2017). doi:10.1002/ejic.201700657.

[23] E.A. Juban, J.K. McCusker, Ultrafast dynamics of 2E state formation in Cr(acac)3, J. Am. Chem. Soc. 127 (2005) 6857–6865. doi:10.1021/ja042153i.

[24] E.M.S. Maçôas, R. Kananavicius, P. Myllyperkiö, M. Pettersson, H. Kunttu, Relaxation Dynamics of Cr(acac) 3 Probed by Ultrafast Infrared Spectroscopy, J. Am. Chem. Soc. 129 (2007) 8934–8935. doi:10.1021/ja071859k.

[25] J.N. Schrauben, K.L. Dillman, W.F. Beck, J.K. McCusker, Vibrational coherence in the excited state dynamics of Cr(acac)3: probing the reaction coordinate for ultrafast intersystem crossing, Chem. Sci. 1 (2010) 405. doi:10.1039/c0sc00262c.

[26] H. Ando, S. Iuchi, H. Sato, Theoretical study on ultrafast intersystem crossing of chromium(III) acetylacetonate, Chem. Phys. Lett. 535 (2012) 177–181. doi:10.1016/j.cplett.2012.03.043.

[27] E.M.S. Maçôas, S. Mustalahti, P. Myllyperkiö, H. Kunttu, M. Pettersson, Role of vibrational dynamics in electronic relaxation of Cr(acac)3, J. Phys. Chem. A. 119 (2015) 2727–2734. doi:10.1021/jp509905q.

[28] V.G. Sala, S. Dal Conte, T.A. Miller, D. Viola, E. Luppi, V. Véniard, G. Cerullo, S. Wall, Resonant optical control of the structural distortions that drive ultrafast demagnetization in <math> <mrow> <msub> <mi>Cr</mi> <mn>2</mn> </msub> <msub> <mi mathvariant="normal">O</mi> <mn>3</mn> </msub> </mrow> </math>, Phys. Rev. B. 94 (2016) 14430. doi:10.1103/PhysRevB.94.014430.

[29] M. Cammarata, R. Bertoni, M. Lorenc, H. Cailleau, S. Di Matteo, C. Mauriac, S.F. Matar, H. Lemke, M. Chollet, S. Ravy, C. Laulhé, J.-F. Létard, E. Collet, Sequential Activation of Molecular Breathing and Bending during Spin-Crossover Photoswitching Revealed by Femtosecond Optical and X-Ray Absorption Spectroscopy, Phys. Rev. Lett. 113 (2014) 227402. doi:10.1103/PhysRevLett.113.227402.

[30] R. Field, L.C. Liu, W. Gawelda, C. Lu, R.J.D. Miller, Spectral Signatures of Ultrafast

Spin Crossover in Single Crystal [FeII(bpy)3](PF6)2, Chem. - A Eur. J. 22 (2016) 5118–5122. doi:10.1002/chem.201600374.

[31] A.M. Brown, C.E. McCusker, J.K. McCusker, Spectroelectrochemical identification of charge-transfer excited states in transition metal-based polypyridyl complexes, Dalt. Trans. 43 (2014) 17635–17646. doi:10.1039/C4DT02849J.

[32] S. Ohkoshi, M. Mizuno, G. Hung, K. Hashimoto, Magnetooptical Effects of Room Temperature Molecular-Based Magnetic Films Composed of Vanadium Hexacyanochromates, J. Phys. Chem. B. 104 (2000) 9365–9367. doi:10.1021/jp002002b.

[33] S.E. Greenough, G.M. Roberts, N.A. Smith, M.D. Horbury, R.G. McKinlay, J.M. Żurek, M.J. Paterson, P.J. Sadler, V.G. Stavros, S.E. Bradforth, M.N.R. Ashfold, J. Moan, P. Mroz, D. Nowis, J. Piette, B.C. Wilson, J. Golab, Ultrafast photo-induced ligand solvolysis of cis-[Ru(bipyridine) $_2$ (nicotinamide) $_2$] $^{2+}$: experimental and theoretical insight into its photoactivation mechanism, Phys. Chem. Chem. Phys. 16 (2014) 19141–19155. doi:10.1039/C4CP02359E.

[34] S.E. Greenough, M.D. Horbury, J.O.F. Thompson, G.M. Roberts, T.N. V. Karsili, B. Marchetti, D. Townsend, V.G. Stavros, C. Jouvet, S.E. Bradforth, M.N.R. Ashfold, Solvent induced conformer specific photochemistry of guaiacol, Phys. Chem. Chem. Phys. 16 (2014) 16187. doi:10.1039/C4CP02424A.

[35] J.J. Snellenburg, S.P. Laptenok, R. Seger, K.M. Mullen, I.H.M. van Stokkum, Glotaran : A Java -Based Graphical User Interface for the R Package TIMP, J. Stat. Softw. 49 (2012) 1–22. doi:10.18637/jss.v049.i03.